

Doppler-free resonantly enhanced two-photon spectroscopy of np and nf Rydberg states in atomic cesium

Craig J. Sansonetti* and C.-J. Lorenzen†

National Measurement Laboratory, National Bureau of Standards, Gaithersburg, Maryland 20899.

(Received 14 February 1984)

The fine-structure intervals of selected np ($n=18-83$) and nf ($n=14-28$) Rydberg states in neutral Cs have been measured by Doppler-free resonantly enhanced two-photon laser spectroscopy with a thermionic diode detector. One cw dye laser was tuned near resonance with a $6s-5d$ electric quadrupole transition while a second was scanned through the relevant $5d-np, nf$ transitions. This is the first Doppler-free study of these series by strictly optical methods. The experimental fine-structure intervals are in good agreement with splitting formulas derived by other authors from fine-structure measurements of lower-lying np and nf levels. Our results and the best previous data have been fitted with several expressions that have been used or suggested for the representation of fine-structure data. A recently proposed expansion formula including inverse even powers of the effective quantum number is found to have little practical significance for the description of experimental intervals.

I. INTRODUCTION

In recent years there has been great interest in the measurement of energies, fine- and hyperfine-structure intervals, and isotope shifts of atomic Rydberg states. Particularly extensive studies have been made for the ns and nd series of the alkali-metal atoms.¹ These series can be observed by Doppler-free nonresonant two-photon absorption from the ground state at wavelengths readily produced by cw dye lasers. Although the transition rates for such two-photon processes are very small (of the order of 100 s^{-1}), they can be observed to high principal quantum numbers with excellent signal-to-noise ratio by using a thermionic diode detector.² By contrast, there have been few investigations of the np , nf , and higher angular momentum series of the alkali metals by optical methods because these states are not accessible by equally convenient experimental techniques.

In this experiment we have demonstrated the utility of resonantly enhanced two-photon spectroscopy in combination with the thermionic diode detector for observing the np and nf series of atomic Cs. The detailed theory of this experimental method has been given by Bjorkholm and Liao.³ Although two-photon transitions of the type $6s-np, nf$ are forbidden by electric-dipole selection rules, it is possible to observe such transitions in Cs because of the weak electric-quadrupole coupling of the $6s$ and $5d$ levels. By using two lasers of unequal frequencies such that one of the 5^2D levels serves as a nearly resonant intermediate state, a very large enhancement of the transition rates can be obtained so that the two-photon transitions can be readily induced. A similar dipole-quadrupole two-photon method was used by Liao and Bjorkholm to measure the $4f$ fine structure in Na.⁴ Here we apply the method to measure fine-structure intervals of Cs np and nf Rydberg states.

II. EXPERIMENT

The experimental arrangement we used to measure the fine-structure splitting of the $np^2P_{1/2,3/2}$ and $nf^2F_{5/2,7/2}$ states of Cs is shown in Fig. 1. A thermionic diode containing Cs vapor served as both absorption cell and as a very sensitive detector of atoms excited into Rydberg states.² In its simplest form such a diode consists of a directly heated cathode filament surrounded by a cylindrical anode. The diode is operated in the space-charge-limited mode. When an atom is excited into a Rydberg state, its radiative lifetime is long and there is a high probability that it will be collisionally ionized. The ion so produced is trapped in the space charge causing an increase of the diode current which is readily detected. Because the recombinative lifetime of the ion in the space

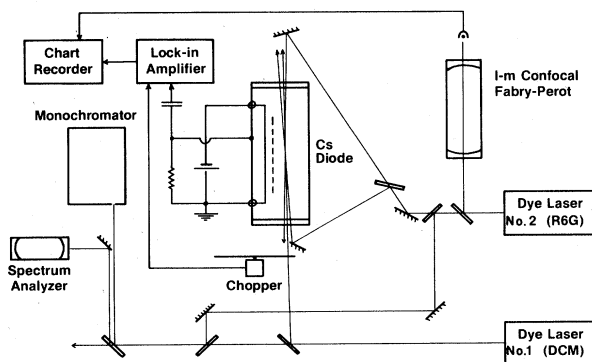


FIG. 1. Experimental apparatus for measuring fine-structure intervals in a Cs thermionic diode by Doppler-free resonantly enhanced two-photon spectroscopy.

charge is quite long, the diode displays a high internal amplification.

In the initial stages of this work our thermionic diode consisted of a stainless-steel hot-pipe bisected axially by a grid of stainless-steel wire. One half of the pipe contained a directly heated tungsten filament while the other half was used as a field-free excitation region shielded by the wire grid. The signal was taken directly from the wall of the hot-pipe, which served as the anode. This diode was operated with no external bias voltage. The pipe was heated to produce a Cs vapor pressure of approximately 5 mTorr and was filled with 30 mTorr of Ne buffer gas. All of the nf intervals were measured with this system.

The hot-pipe diode was later replaced by a sealed glass diode similar to that described by Harvey.² This diode was operated with no buffer gas at Cs vapor pressures of less than 1 mTorr and was externally biased to suppress residual fields in the excitation region and so minimize Stark effect in the np states with very high n . For both diode systems the signal was observed across a 10-k Ω load resistor and detected by a lock-in amplifier after being decoupled by a 0.47- μ F capacitor. Chopping frequencies between 10 and 30 Hz were used. Small parts of the laser beams were sent to a spectrum analyzer and a 0.5-m monochromator for approximate wavelength calibration.

The light beams from two frequency-stabilized cw dye lasers (linewidths 1–2 MHz) were directed to copropagate or counterpropagate through the thermionic diode. The first laser [dye, 4-dicyanomethylene-2-methyl-6-*p*-dimethylaminostyryl-4*H*-pyran (DCM); power, 90 mW] was chopped and tuned near resonance with either the $6^2S_{1/2}-5^2D_{3/2}$ or the $6^2S_{1/2}-5^2D_{5/2}$ quadrupole transition at 14 499 or 14 596 cm^{-1} , respectively. Although these two transitions have oscillator strengths of only 3.28×10^{-7} ($6s-5D_{3/2}$) and 5.65×10^{-7} ($6s-5D_{5/2}$),⁵ the Doppler-broadened quadrupole lines can be detected with the diode. This facilitates tuning to the transitions. The second laser (dye: Rhodamine 6G) was scanned through the $5d-np$ and $5d-nf$ resonances. A small part of this yellow laser beam was sent through a pressure-tight 1-m confocal Fabry-Perot interferometer with a free spectral range of 74.71(4) MHz for relative frequency calibration of the recorded spectra. To avoid saturation, the yellow laser power at the Cs diode was attenuated with neutral density filters to approximately 100 μ W for the $5d-np$ and 10 μ W for the $5d-nf$ transitions.

Although the production of Doppler-free spectra in nonresonant two-photon spectroscopy with counterpropagating beams is well known, the mechanism by which Doppler-free spectra are produced in resonantly enhanced two-photon spectroscopy may be less apparent. The principle of the method can be understood by a simple physical argument which views the process as a sequential two-step excitation. The first laser is absorbed by only those atoms for which the initial-to-intermediate-state transition frequency is Doppler shifted into resonance with the laser frequency. As a consequence, the atoms excited to the intermediate state all have the same velocity parallel to the laser beam. If the second laser beam propagates parallel or antiparallel to the first, the atomic popu-

lation that it probes is similar to that in an atomic beam in that it has a uniform though not necessarily zero velocity along the laser beam. The second laser interacts with this velocity selected population only when it is resonant with the Doppler shifted intermediate-to-final-state transition frequency.

In our excitation scheme ($6s-5d-np, nf$) only the $5d$ intermediate state has hyperfine structure comparable in size to the fine-structure intervals of interest.⁶ By contrast, the $6s$ ground state has a hyperfine-structure interval of 9.2 GHz allowing selective excitation out of the $F=3$ or $F=4$ component, while the np or nf Rydberg states have negligible hyperfine splitting. When the yellow laser is scanned through a $5d-np$ or $5d-nf$ transition, a Doppler-free resonance is observed for each hyperfine component of the $5d$ state. The spacing of the observed components is determined by the unequal Doppler shifts for the red (f_r) and yellow (f_y) laser frequencies.³ For copropagating laser beams the Doppler shifts add and the observed spacings are expanded by a factor of $(f_r + f_y)/f_r$ from the actual $5d$ intervals. For counterpropagating beams the Doppler shifts nearly cancel and the observed spacings are contracted by the factor $(f_r - f_y)/f_r$. Note that this factor is negative in the case of interest here, hence our spectra with counterpropagating beams display the $5d$ hyperfine components in inverted order. These characteristics of the experimental method are illustrated in Figs. 2 and 3. The fine structure of the np and nf lev-

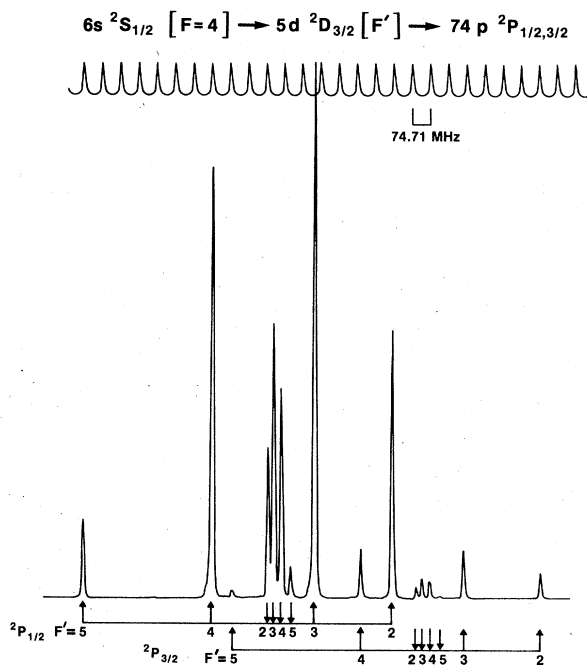


FIG. 2. Recorded spectrum of the $6s-5d-74p$ transition with simultaneous copropagating and counterpropagating beams. The resonances due to the copropagating beams are identified with erect arrows and those due to the counterpropagating beams with inverted arrows. The frequency of the laser scanning the $5d-74p$ transition increases to the right.

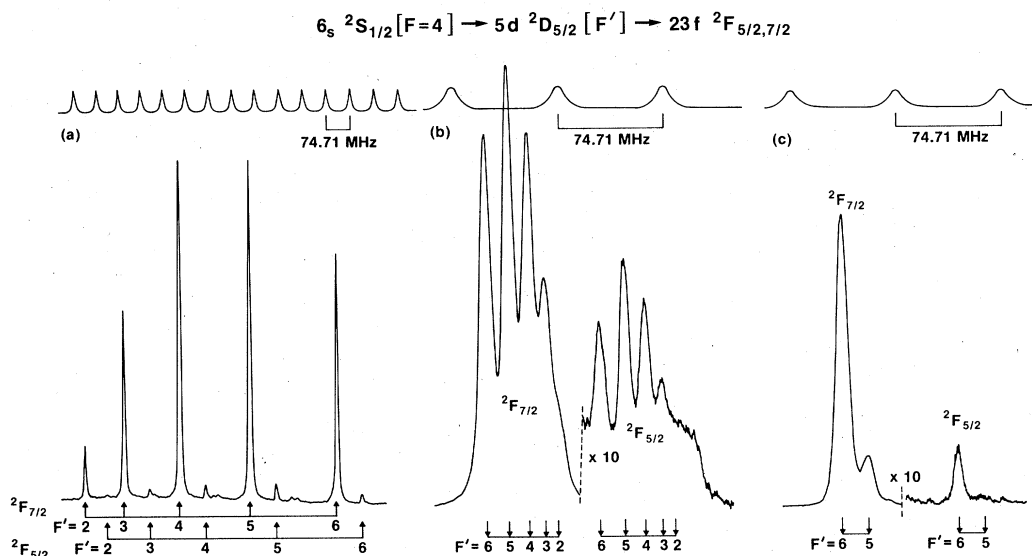


FIG. 3. Recorded spectra of the $6s$ - $5d$ - $23f$ transition. The frequency of the second (Rhodamine-6G) laser increases to the right. (a) Trace recorded with copropagating laser beams. (b) Trace recorded with counterpropagating laser beams. Note that for higher values of n the $5d$ hyperfine-structure patterns associated with the ${}^2F_{5/2}$ and ${}^2F_{7/2}$ levels will overlap. (c) Trace recorded with the first (DCM) laser tuned 1 GHz to the red wing of the $6s$ - $5d$ transition. This simplifies the spectrum by increasing the intensity of the $F'=6$ component with respect to the rest of the intermediate state hyperfine components. See text.

els appears unaltered in the recorded spectra.

All of the intervals reported in this work were measured using both copropagating and counterpropagating beams. When $5^2D_{3/2}$ was used as the intermediate state, it was generally possible to record both simultaneously as shown in Fig. 2. In most cases no significant discrepancy that could be correlated with the propagation direction was observed. This demonstrates that systematic error due to monotonic drift of the red-laser frequency was small. In the few cases where a systematic difference was found, the data were discarded and the interval remeasured. When counterpropagating beams and the $5^2D_{5/2}$ intermediate state were used, the contraction of the hyperfine structure led to unresolved components in the recorded spectra. To simplify the spectra it was convenient to tune the red laser about 1 GHz into the blue or red wing of the $6s$ - $5d$ transition. Since the Gaussian Doppler profile of each hyperfine component falls off rapidly with increasing detuning from its line center, the nearest hyperfine component was strongly favored by this procedure and then stood out as a simple sharp profile [Fig. 3(c)].

All of the two-photon resonances observed in the hot-pipe diode showed widths (FWHM) of 10 to 15 MHz. This is substantially greater than would be indicated by natural line widths alone, but it is consistent with the self-broadening rates of Weber and Niemax⁷ assuming a Cs number density of $1 \times 10^{14}/\text{cm}^3$. It is likely that saturation broadening of the $5d$ - nf transitions also contributed significantly to the linewidths. Broadening due to the Ne buffer gas should be negligible at a Ne pressure of 30 mTorr.⁸ The contribution due to the natural width of the $6s$ - $5d$ transition is also negligible. In the glass diode with Cs number densities of less than $2 \times 10^{13}/\text{cm}^3$, the observed widths were typically 6 MHz.

In principle, Stark broadening is an additional possible contributor to the observed linewidths. Both of our thermionic diodes were equipped with shielding grids separating the Cs excitation region from the fields associated with the cathode filament, hence the fields in the excitation region were quite small. We observed no evidence of Stark effect for any of the nf states. For the np states with $n > 60$, asymmetric Stark profiles were evident when the glass diode was operated without external bias. With a properly adjusted bias the residual fields could be reduced sufficiently that no evidence of Stark effect could be seen even at $n = 83$.

The accuracy of fine-structure intervals determined by scanning the yellow-laser frequency, as described above, depends critically on the stability of the red-laser frequency and of the 1-m confocal Fabry-Perot. For this reason the method is best suited to relatively small intervals for which the scan time can be kept short. This limits measurements in the Cs np series to high principal quantum numbers. In order to obtain a few accurate 2P intervals at lower n for this work, we have determined the 18^2P , 25^2P , 33^2P , and 44^2P intervals by measuring and differencing the absolute level values. The technique for measuring absolute energy levels by using the resonant two-photon excitation scheme was developed by K.-H. Weber and C. J. Sansonetti in this laboratory. They are currently making extensive measurements of absolute energy levels in the Cs np and nf series. Details of the experimental method and results will be published elsewhere.

III. RESULTS AND DISCUSSION

We have determined selected Cs I n^2P fine-structure intervals in the range $n = 18$ to 83 and n^2F intervals for

TABLE I. Cs I n^2P fine-structure intervals.

n	This work (MHz)	Literature (MHz)	Calculated ^f —observed (MHz)	Calculated ^g —observed (MHz)
6		16 609 650(40) ^b	17.1	7.3
7		5427 700(50) ^c	-12.9	-9.7
8		2478 530(20) ^c	16.0	-8.6
9		1339 520(30) ^c	-30.8	13.0
10		805 380(30) ^c	-43.6	7.5
11		{ 521 680(80) ^c 521 620(100) ^d	{ -44.7 15.3	{ -3.9 56.1
12		357 130(100) ^d	-64.4	-35.0
13		255 130(100) ^d	-56.3	-36.0
14		188 600(100) ^d	-83.5	-69.7
15		143 270(100) ^d	-25.3	-16.0
16		111 440(100) ^d	-55.7	-49.5
17		88 280(100) ^d	34.2	38.3
18	71 208(5) ^a	71 270(100) ^d	-7.9	-5.3
19		58 270(100) ^d	-32.7	-31.1
20		48 240(100) ^d	-0.3	0.5
21		40 490(100) ^d	-84.5	-84.0
23		29 172.2(4.0) ^e	-1.8	-1.9
25	21 744(5) ^a	21 744.0(1.0) ^e	-1.1	-1.5
26		18 963.2(1.0) ^e	-0.3	-0.7
27		16 636.6(1.0) ^e	0.8	0.3
28		14 676.0(1.0) ^e	1.1	0.5
32		9310.4(1.0) ^e	2.9	2.4
33	8395(5) ^a		0.9	0.4
34		7593.0(1.0) ^e	2.2	1.7
39		4811.2(2.0) ^e	1.1	0.7
42		3775.6(10.0) ^e	-5.1	-4.3
44	3237(5) ^a		1.7	1.3
47	2611(8)		1.8	1.6
50	2135(5)		3.4	3.2
54	1668(6)		0.9	0.7
57	1403(4)		0.3	0.1
61	1127(5)		3.0	2.9
64	969(2)		0.9	0.8
67	839(2)		-0.3	-0.4
71	698(2)		0.1	0.0
74	614(3)		-1.3	-1.4
77	542(2)		-1.4	-1.5
80	480(4)		-0.6	-0.6
83	427(2)		0.1	0.1

^aDetermined by difference of the absolute $^2P_{3/2}$ and $^2P_{1/2}$ levels measured by photographic Fabry-Perot interferometry. See text.

^bReference 11.

^cCalculated from wavelengths given in Ref. 12.

^dReference 13.

^eReference 14.

^fCalculated from fitted empirical formula. See Table IV. Differences are from the observed values in this work where available.

^gCalculated from fitted Pendrill formula. See Table IV. Differences are from the observed values in this work where available.

$n = 14$ and 17 to 28. The results are presented in Tables I and II along with the best literature values for fine-structure splittings in these series. Each reported interval is the average of 12 to 32 independent measurements. The

TABLE II. Cs I n^2F fine-structure intervals.

n	This work (MHz)	Literature (MHz)	Calculated ^d —observed (MHz)	Calculated ^e —observed (MHz)
4		-5438(6) ^a	1.1	1.6
5		-4482(9) ^a	-3.0	1.1
6		-3172(6) ^a	4.3	3.0
7		-2209(9) ^a	-10.0	-11.3
8		-1592(18) ^a	6.5	5.8
9		-1166(21) ^a	4.4	4.2
10		-873.2(2.0) ^b	1.3	1.3
11		-667.2(2.0) ^b	-1.9	-1.8
12		-522.0(3.0) ^b	-1.5	-1.4
13		-416.0(3.0) ^b	-0.8	-0.7
14	-337.5(2.0)	-336.8(1.0) ^b	-0.1	0.0
15		-276.3(1.0) ^b	0.4	0.4
16		-229.3(1.0) ^b	0.5	0.6
17	-190.2(2.9)	-190.5(2.0) ^b	-1.2	-1.2
18	-162.0(1.8)		-0.1	-0.1
19	-138.4(2.6)		0.1	0.0
20	-119.0(1.4)		0.0	0.0
21	-103.8(2.2)		0.8	0.8
22	-90.0(2.2)		0.2	0.2
23	-78.9(1.7)		0.2	0.1
24	-71.0(2.0)	-69.58(2.0) ^c	0.2	0.2
25	-61.7(2.5)		0.2	0.2
26	-54.2(1.6)		-0.5	-0.6
27	-49.3(2.1)		0.4	0.3
28	-43.7(1.6)		-0.2	-0.3
29		-40.32(3.0) ^c	0.7	0.7
30		-36.60(4.0) ^c	0.8	0.8

^aReference 16.

^bReference 6.

^cReference 14.

^dCalculated from fitted empirical formula. See Table IV. Differences are from the observed values in this work where available.

^eCalculated from fitted Chang formula. See Table IV. Differences are from the observed values in this work where available.

estimated uncertainty of each measured value is given in parentheses. This uncertainty includes three times the standard error of the mean of the individual measurements, a contribution from the uncertainty in the free spectral range of our confocal Fabry-Perot interferometer, and a worst case estimate of systematic errors due to thermal drift of the interferometer and drift of the red-laser frequency. For all of the 2F intervals and the smaller 2P intervals, random scatter dominates the uncertainties. For the larger 2P intervals, which require longer scan times, the estimated drift rates are the dominant contributors.

Analytical representations of experimental fine-structure data have frequently been given by fitting the constant coefficients in the empirical formula

$$\Delta_{fs} = A/(n^*)^3 + B/(n^*)^5 + C/(n^*)^7 + \dots \quad (1)$$

by standard least-squares procedures. This formula successfully describes the data in many cases. Aside from its asymptotic $(n^*)^{-3}$ dependence, however, it has no clear

TABLE III. Fitted formulas for the np and nf effective quantum numbers n^* , $n^* = n_\infty^* - a/(n_\infty^*)^2 - b/(n_\infty^*)^4 - c/(n_\infty^*)^6$, where $n_\infty^* = n - \epsilon_\infty$.

	$n^2P_{\text{cog}}^a$	$n^2P_{1/2}^b$	$n^2F_{\text{cog}}^c$
ϵ_∞	3.569 902(1)	3.591 5664(35)	0.033 479(5)
a	0.373 32(20)	0.363 02(14)	-0.191 44(7)
b	0.348(4)	0.3667(17)	-0.044(20)
c	1.274(20)	1.1320(59)	3.09(26)

^aBased on data from Refs. 11, 13, and 14. The values of n^* calculated from these coefficients should not be used to calculate level energies.

^bBased on experimental levels from Refs. 11, 12, and 13. The values of n^* calculated from these coefficients can be used with the series limit 31 406.4702 cm^{-1} to calculate the energies of the $n^2P_{1/2}$ levels for $n \geq 6$.

^cBased on data from Ref. 14 and K. B. S. Eriksson and I. Wenaker, Phys. Scr. 1, 21 (1970). The values of n^* calculated from these coefficients should not be used to calculate level energies.

theoretical interpretation. Two alternative formulas have recently been suggested as better founded in atomic theory. The first was proposed by Chang⁹ who developed the expression

$$\Delta_{fs} = \{ [(n+l)!/(n-l-1)!] \times (A + B/n^2 + C/n^4 + \dots) \} / n^{2l+4} \quad (2)$$

based on a perturbation calculation using hydrogenic wave functions. This expression has the considerable advantage of depending only on the principal quantum number and not on the effective quantum number. The second alternative expression

$$\Delta_{fs} = A/(n^*)^3 + B/(n^*)^4 + C/(n^*)^5 + D/(n^*)^6 + \dots \quad (3)$$

was derived by Pendrill¹⁰ from the Rydberg-Ritz term formula which can be justified theoretically and which is known to represent series of absolute energy levels with high accuracy.

We have performed a weighted least-squares fit of each of these formulas to the best n^2P and n^2F fine-structure data. The resulting coefficients are summarized in Tables

III and IV and the residuals of the fitted formulas for each series are given with the experimental data in Tables I and II. The results for the individual series are discussed separately below.

A. n^2P intervals

Our experimental fine-structure intervals for the n^2P levels are summarized in Table I along with the most accurate available results for all other n^2P states including values from Eriksson *et al.*¹¹ ($n=6$), Sansonetti¹² ($n=7-11$), Lorenzen and Niemax¹³ ($n=11-21$), and Goy *et al.*¹⁴ ($n=23-42$). The values for $n < 11$ are based on wavelengths measured in emission sources. The cited intervals for $n=12-21$ are differences of the absolute $^2P_{3/2}$ and $^2P_{1/2}$ energies as measured by Lorenzen and Niemax¹³ with a frequency-doubled dye laser in a Cs thermionic hot-pipe diode. The results of Goy *et al.*,¹⁴ which are the most precise values that have been reported for this series, were obtained in an optical-radio frequency double-resonance experiment. Our work represents the first Doppler-free observation of this series by optical methods and extends the measured fine-structure intervals to much higher principal quantum numbers than have previously been observed.

Goy *et al.*¹⁴ have fitted their fine-structure data using the empirical expression in Eq. (1) with three constants. Extrapolation with their formula to higher values of n gives results which are in excellent agreement with our data. Application of the formula at low n , however, gives results that disagree with the best data by far more than their estimated uncertainties. For this reason we attempted to make a new fit of Eq. (1) to all of the best data.

It was first necessary to determine appropriate values of n^* to be used in the fitting. For the empirical formula it is customary to use n^* for the centers of gravity of the fine-structure doublets. Experimental energy levels from Ref. 11 ($n=6$) and Ref. 13 ($n=7-21$) were used to determine the 2P centers of gravity for these levels. For $n > 21$ the 2P centers of gravity were calculated from the quantum defect formulas of Goy *et al.*¹⁴ and the Cs ionization energy 31 406.471 0(7) cm^{-1} given by Lorenzen and Niemax.¹⁵ The center-of-gravity values of n^* were then fit to a series formula as shown in Table III, and the results of this formula were used in fitting the fine-structure data.

TABLE IV. Fitted formulas for the n^2P and n^2F fine-structure intervals. All coefficients are given in MHz.

	n^2P		n^2F	
	Empirical ^a	Pendrill ^b	Empirical ^a	Chang ^c
A	$2.14054(5) \times 10^8$	$2.140 10(6) \times 10^8$	$-9.752(7) \times 10^5$	$-9.784(8) \times 10^5$
B	$-4.198(22) \times 10^7$	$-1.285(8) \times 10^7$	$1.128(5) \times 10^7$	$-3.08(7) \times 10^6$
C	$2.468(30) \times 10^8$	$-4.542(30) \times 10^7$	$-2.00(6) \times 10^7$	$1.02(9) \times 10^7$
D	$2.05(11) \times 10^8$			
E		$2.8692(70) \times 10^8$		

^a $\Delta_{fs} = A/(n^*)^3 + B/(n^*)^5 + C/(n^*)^7 + D/(n^*)^9$. Use center-of-gravity n^* from Table III.

^b $\Delta_{fs} = A/(n^*)^3 + B/(n^*)^4 + C/(n^*)^5 + D/(n^*)^6 + E/(n^*)^7$. Reference 10. Use $^2P_{1/2}n^*$ from Table III.

^c $\Delta_{fs} = \{ [(n+l)!/(n-l-1)!] (A + B/n^2 + C/n^4) \} / n^{2l+4}$. Reference 9.

We found that Eq. (1) with three constants was not adequate to describe the experimental 2P intervals at low n . Addition of a fourth constant [i.e., a term with $1/(n^*)^9$] was required to fit the data for $n=6-9$. With this additional term a good representation was obtained for the entire series. The fitted constants are given in Table IV.

We have also tested the two alternative formulas, Eqs. (2) and (3), to assess their usefulness for representing the experimental data. We could not fit the 2P fine-structure data using the formula of Chang⁹ regardless of how many terms of the expansion were used. This result was expected since Chang states that his derivation is not applicable to strongly penetrating series. Fitting the formula of Pendrill¹⁰ produced more interesting results.

Although it is not stated in Pendrill's paper, a careful examination of his derivation indicates that his expressions for the coefficients in the fine-structure formula are valid if the intervals are fitted as a function of the effective quantum number for the lower of the doublet levels. We have determined the necessary effective quantum numbers by fitting the modified Ritz formula to the ${}^2P_{1/2}$ levels of Refs. 11 ($n=6$), 12 ($n=7,8$), and 13 ($n>8$). The coefficients given in Table III accurately reproduce all of the experimental data for $n\geq 6$. The Ritz formula published by Lorenzen and Niemax¹⁶ for this series was not used because it does not represent the experimental levels well for $n=7$ and 8.

We first determined that no satisfactory fit to the 2P intervals was possible without the inclusion of the third, fifth, and seventh powers of $1/(n^*)$ regardless of what even powers were included. Taking all terms in the Pendrill formula up to the seventh power produced a formula that represented the data well, but the calculated coefficient of the sixth power had an uncertainty greater than its value. By omitting the sixth power a formula which described the data equally well and in which all coefficients were well defined was obtained. The coefficients for this expression are given in Table IV.

One of the attractive features of Pendrill's derivation is that it relates the expansion coefficients of Eq. (3) to the coefficients of the Rydberg-Ritz term formula. Based on the Ritz coefficients of Goy *et al.*,¹⁴ Pendrill has made predictions for the coefficients of Eq. (3) which can be compared directly to our experimental values.¹⁰ The predicted value $A=2.138(4)\times 10^8$ MHz is in agreement with the fitted value $2.140(6)\times 10^8$ MHz. This is not surprising since A alone determines the fine-structure intervals in the limit of high n . In this limit Pendrill's expression for A is readily apparent. The predicted value $B=-1.042(4)\times 10^7$ MHz is 20% smaller than the fitted value $-1.285(8)\times 10^7$ MHz, and the predicted value $C=-2(3)\times 10^7$ MHz differs substantially from the experimental value $-4.542(30)\times 10^7$ MHz although there is agreement within the large uncertainty of the prediction.

On the basis of the above comparisons the predictions of Pendrill are qualitatively confirmed. In particular, the $(n^*)^{-4}$ term which is not included in the empirical formula does play an important role in representing the experimental data. This term is less important, however, if the fine-structure intervals are fitted with respect to the effective quantum number for the doublet center of gravity. It

is possible to derive Pendrill's formula to conform to this convention.¹⁷ If this is done, the expression for the A coefficient is unchanged, but the expression for the B coefficient is multiplied by a factor of $-1/(2j+2)$, where j is the smaller of the doublet J values. For a 2P series the effect of fitting with respect to the center-of-gravity effective quantum number is to reduce the magnitude of the $(n^*)^{-4}$ dependence by a factor of 3. With this reduction, and the low accuracy of fine-structure data at low n , it is not surprising that the empirical expansion in odd powers only has been sufficient to represent most experimental data.

For the case of the precise data of Goy *et al.*¹⁴ for the Cs 2P series in the vicinity of $n=30$, Pendrill has suggested that the $(n^*)^{-4}$ term should contribute much more to the fine-structure interval than the $(n^*)^{-5}$ term.¹⁰ In fact, Goy *et al.* fitted their fine-structure data as a function of the average quantum defect for the doublet. By using the procedure of Pendrill's derivation it is easy to show that if the average quantum defect is chosen as the independent variable the coefficient of the $(n^*)^{-4}$ term vanishes.

B. n^2F Intervals

In Table II the present data for the fine-structure splitting of the n^2F levels are listed together with the data of Sansonetti and Andrew¹⁸ ($n=4-9$), Fredriksson *et al.*⁶ ($n=10-17$), and Goy *et al.*¹⁴ ($n=24,29,30$). Our results confirm that these intervals are inverted and show an asymptotic $1/(n^*)^3$ dependence which indicates that they will remain inverted for all higher n . As in the case of the n^2P series, the formula given by Goy *et al.* accurately predicts our new data but does not give good results for low n . We have made a new fit with Eq. (1) including all of the best data and using values of n^* from the expansion in Table III. The coefficients are given in Table IV. The resulting formula is in exact agreement with that given by Sansonetti and Andrew from fitting the data for the $n=4-17$ levels only.

We have also fit the formulas of Pendrill¹⁰ and Chang⁹ to the n^2F fine-structure data. In fitting the Pendrill formula the coefficients of all terms with inverse even powers of n^* are ill defined ($>90\%$ uncertainty), hence the Pendrill formula has no advantage over the empirical formula for this series. The formula of Chang with three terms gives a representation of the data that is as satisfactory as the empirical formula. The coefficients for this formula are also given in Table IV. The Chang formula is more convenient than the empirical formula because it requires only the principal quantum number and not the effective quantum number. Success with these data, however, is not a good test of the validity of the formula. The quantum defects for this series are small enough that a simple expansion in odd inverse powers of n can represent the data within their experimental uncertainties.

IV. CONCLUSIONS

We have used Doppler-free resonantly enhanced two-photon spectroscopy to measure the fine-structure intervals of np and nf Rydberg states in Cs. Our highly sensitive thermionic diode detector made it possible for us to

use the $5d$ levels, which are only weakly electric-quadrupole coupled to the ground state, as resonant intermediate states. This technique makes it possible to study states of odd parity and to induce $\Delta l = 1$ or 3 transitions to high Rydberg states with two optical photons. The resulting spectra show excellent signal-to-noise ratio and can be obtained at very low Cs number density. Our measured fine-structure intervals, which for the n^2P series extend the range of experimental values to $n = 83$, are in good agreement with extrapolations from previous measurements at lower n .

We have investigated the application of three formulas which have been used to represent fine-structure intervals to all of the best data for the Cs n^2P and n^2F intervals. Both series can be described satisfactorily by the empirical expansion in odd inverse powers of n^* . The n^2F data is also represented well by the formula of Chang⁹ which is derived by a perturbation treatment with hydrogenic wave functions. The formula of Pendrill,¹⁰ which is derived from the extended Ritz formula and includes inverse even powers of the effective quantum number, is supported by the data for the n^2P series. We find, however, that the importance of the even powers in the expansion depends critically on which effective quantum numbers are used as the independent variable. If n^* for one of the individual

series is used the inclusion of even powers is quite important. If the center-of-gravity effective quantum number is used the dependence is reduced, and if the average effective quantum number is used the dependence on $(n^*)^{-4}$ vanishes. Although the formula of Pendrill is confirmed in a formal sense, it has no practical advantage over the empirical formula in representing experimental intervals at the current level of accuracy.

ACKNOWLEDGMENTS

K.-H. Weber provided the glass thermionic diode used for much of this work and helped with the measurement of the 18^2P , 25^2P , 33^2P , and 44^2P intervals by photographic Fabry-Perot interferometry. His contributions are gratefully acknowledged. We are indebted to W. D. Phillips and L. J. Moore for loans of equipment essential to carrying out this experiment, to D. K. Kahaner for help in developing the weighted least-squares fitting routines, and to L. R. Pendrill for helpful comments which increased our understanding of his formula. One of us (C.-J.L.) gratefully acknowledges the financial support of the Deutsche Forschungsgemeinschaft and the National Bureau of Standards.

*On assignment from Department of Physics, Purdue University, West Lafayette, IN 47907.

†On assignment from Institut für Experimentalphysik der Universität Kiel, Olshausenstrasse 40-60, D-2300 Kiel 1, Federal Republic of Germany. Present address: Fried. Krupp GmbH, Krupp Forschungsinstitut, Muenchener Strasse 100, D-4300 Essen 1, Federal Republic of Germany.

¹See, for example, C. -J. Lorenzen, K. Niemax, and L. R. Pendrill, *Opt. Commun.* **39**, 370 (1981); K. C. Harvey and B. P. Stoicheff, *Phys. Rev. Lett.* **38**, 537 (1977); K. Niemax and L. R. Pendrill, *J. Phys. B* **13**, L461 (1980).

²K. C. Harvey, *Rev. Sci. Instrum.* **52**, 204 (1981); K. Niemax, *Acta Phys. Pol. A* **61**, 517 (1982).

³J. E. Bjorkholm and P. F. Liao, *Phys. Rev. A* **14**, 751 (1976).

⁴P. F. Liao and J. E. Bjorkholm, *Phys. Rev. Lett.* **36**, 1543 (1976).

⁵K. Niemax, *J. Quant. Spectrosc. Radiat. Transfer* **17**, 125 (1977).

⁶K. Fredriksson, H. Lundberg, and S. Svanberg, *Phys. Rev. A* **21**, 241 (1980).

⁷K. -H. Weber and K. Niemax, *Opt. Commun.* **28**, 317 (1979).

⁸W. L. Brillet and A. Gallagher, *Phys. Rev. A* **22**, 1012 (1980).

⁹T. N. Chang, *J. Phys. B* **11**, L583 (1978); T. N. Chang and F. Larijani, *ibid.* **13**, 1307 (1980).

¹⁰L. R. Pendrill, *Phys. Scr.* **27**, 371 (1983).

¹¹K. B. Eriksson, I. Johansson, and G. Norlen, *Ark. Fys.* **28**, 233 (1964).

¹²Intervals calculated from CsI wavelengths given in C. J. Sansonetti, Ph.D. thesis, Purdue University, 1981, available from University Microfilm International, Ann Arbor, MI 48106. Order No. 8200721.

¹³C.-J. Lorenzen and K. Niemax (private communication).

¹⁴P. Goy, J. M. Raimond, G. Vitrant, and S. Haroche, *Phys. Rev. A* **26**, 2733 (1982).

¹⁵C. -J. Lorenzen and K. Niemax, *Z. Phys. A* **311**, 249 (1983).

¹⁶C. -J. Lorenzen and K. Niemax, *Z. Phys. A* **315**, 127 (1984).

¹⁷L. R. Pendrill (private communication).

¹⁸C. J. Sansonetti and K. L. Andrew, *Phys. Rev. A* **22**, 1370 (1980).